Proceedings of the 29th Annual Conference of the Computational Fluid Dynamics Society of Canada
CFDSC2021
July 27-29, 2021, Online

Outlet loss in Archimedes screw generators

Scott Simmons, Amir Aliabadi, William David Lubitz *(Corresponding Author)*
School of Engineering
CEPS, University of Guelph
Guelph, Canada
wlubitz@uoguelph.ca

Guilhem Dellinger
ICube Laboratory
ENGEES
Strasbourg, France

***Abstract*—**Design optimization of Archimedes screw generators for hydropower production relies on performance predicting models. Current power predicting models lack accuracy in various power loss modules. Outlet loss models are the focus of this article. Current outlet loss modelling techniques for Archimedes screw generators lack robust validation and seem to overpredict power loss in cases of low-level submergence. A computational fluid dynamic model was developed by the authors and used to provide valuable data and insight to the literature for future outlet loss model development and validation. Seven different geometrically identical, scale-sized screws were simulated to gather data for this study. It was found that outlet loss scaled by the rotation speed and the outer diameter to the power of four (i.e. the fourth order length-scale divided by the timescale).

Keywords-Archimedes screw generator, hydrodynamic screw, reverse Archimedes screw, hydropower, micro hydropower, run-of-river, renewable energy

I. INTRODUCTION

Archimedes screw generators (ASGs) are an eco-friendly micro-hydropower technology that can help diversify our clean energy production network in Canada. Hundreds of ASG powerplants have been successfully installed and operated globally, mostly in Europe. Archimedes screws were used as pumps since antiquity, and have found use as a generator since the early 1990's [1]. Many screw manufacturers began producing the technology for hydropower generation after more than a century of screw pump production; as such, Archimedes screw design has been largely experience-based. Figure 1 demonstrates the dimensions and parameters used to describe Archimedes screws.

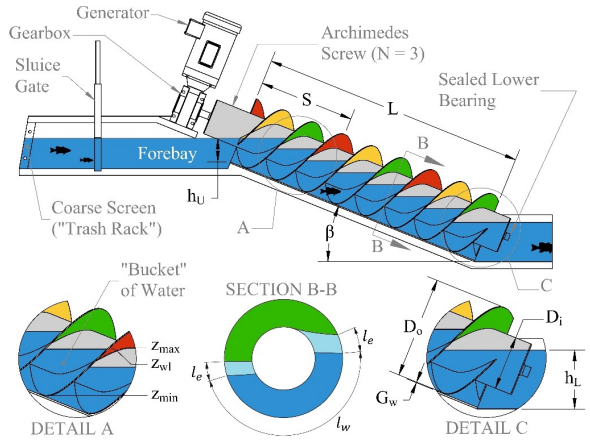

Figure 1. Archimedes screw dimensions and parameters.

Generally, screws are described by their inner and outer diameters (D_i and D_o, respectively), pitch (S), flighted length (L), inclination angle (β), number of blades (N), and gap width (G_w). When operating as a generator, the screw produces power from an available flow rate (Q) across the head (ΔH) at the site. Water enters the top of the screw at the upper water level (h_U) and stats to fill the volume between the blades and trough at the screw's inlet. Once fully formed, the volume of water entrapped between successive blades is termed a "bucket". Detail A in Figure 1 demonstrates the variables used to describe the fill level of a bucket. The local water level in a bucket (z_{wl}) may be non-dimensionalised with the minimum and maximum levels (z_{min} and z_{max}, respectively) of water possible in the bucket. The variable z_{max} is defined as the maximum amount of water that can fill a bucket without spilling over the central cylinder of the screw into the next bucket. The non-dimensional fill height ratio may be calculated as:

$$f = \frac{z_{wl} - z_{min}}{z_{max} - z_{min}} \tag{1}$$

So, a fill height of $f = 1$ would correspond to a bucket that is full to the maximum point before overflowing into the next bucket of the screw. Fill heights higher than unity signify the screw is operating in the overflow regime.

Water translates along the length of the screw in buckets. The blades of the screw convert the pressure (mostly hydrostatic) in the buckets into rotational mechanical energy that is then converted with a gearbox and generator into electrical energy. After translating along the length of the screw, the buckets empty into the lower water level (h_L).The outlet of the screw, and the water level at the outlet of the screw drive significant power loss during operation. To

optimize ASG design, outlet loss needs to be accurately quantified and modelled in the literature. Predictive models may be used to determine site-specific optimal power plant designs.

Design optimization appears to occur in-house with major screw manufacturers since there is a lack of literature on the subject. Some power production [2]–[4] and power loss [2], [4]–[7] models have been presented in the literature; however, a lack of experimental data in the literature has not allowed for robust model development and evaluation. This article will focus on introducing valuable data and analysis to the literature for outlet loss model development.

Current outlet loss modelling techniques calculate outlet loss as a summation of outlet expansion loss and outlet submersion loss. Outlet expansion loss is currently based on Borda-Carnot entrance relationships:

$$P_{L_{OE}}=\rho Q\zeta_L\frac{v_t^2}{2} \tag{2}$$

The outlet expansion loss (P_{LOE}) is a function of the working fluid density (ρ), flow rate (Q), the transport velocity of the screw (v_t), and the Borda-Carnot exit loss coefficient (ζ_L). The transport velocity is the velocity that a bucket translates down the length of the screw, it may be calculated as:

$$v_t=\frac{\omega S}{2\pi} \tag{3}$$

Where it is a function of the rotation speed of the screw (ω) and the pitch.

Outlet submersion loss is based on two cases [2]. When a bucket exits the bottom of the screw, if the lower water level (i.e. h_L) is higher than the bucket, water will flow from the exit channel back into the screw. This is termed the high-level outlet submersion loss case. If the exit channel's water level is lower than the final bucket's water level, the final bucket will empty prematurely due to a lack of back-pressure. This is called the low-level outlet submersion case. Nuernbergk [2] defined outlet submersion loss for ASGs operating with bucket fill heights of $f = 1$. To define the case, the optimal lower water level is defined for a screw with $f = 1$, as:

$$h_L'=\left(\frac{D_o+D_i}{2}\right)\sqrt{1-\left(\frac{S\tan\beta}{\pi D_i}\right)^2}\cos\beta-\frac{S}{N}\sin\beta \tag{4}$$

It is a function of the inner and outer diameters, pitch, inclination angle, and number of blades. It is common to cast the lower water level as a dimensionless submergence level with respect to the top of the screw blade's outer diameter (cf. Detail C in Figure 1).

The submersion loss cases are defined with respect to the optimal lower water level. When $h_L > h_L'$ (i.e. high-level), outlet submersion loss (P_{LOS}) is currently calculated as:

$$P_{L_{OS}}=\rho gQ\frac{\left(h_L-h_L'\right)^2}{h_L} \tag{5}$$

When $h_L < h_L'$ (i.e. low-level), outlet submersion loss (P_{LOS}) is currently calculated as:

$$P_{L_{OS}}=\rho gQ\frac{\left(h_L-h_L'\right)^2}{h_L'} \tag{6}$$

In both cases, submersion loss is a function of the working fluid density, gravitational acceleration, flow rate, the lower water level, and the optimal lower water level. The main difference is the denominator term: in the high-level case the lower water level is used rather than the optimal lower water level.

Outlet submersion losses are larger than expansion losses. Both models have been tested against experimental data [8]. Experiments demonstrated that power output varied significantly with changing lower water level. Experiments and field data suggested that the current submersion model overpredicts power loss in the low-level case; however, it was not possible to directly measure outlet loss experimentally. As well, the majority of data was from laboratory-scale experimentation with $D_o \approx 0.30$ m screws – real world installations are commonly $D_o > 1$ m, with many in the range of 2 m to 3 m, and one installation at Linton Lock, UK as large as $D_o = 5$ m. Therefore, there is a need to expand the dataset used for model evaluation, and, to directly quantify outlet losses. A computational fluid dynamic (CFD) model was developed to accomplish this task.

The main objective of this study was to quantify outlet losses, observe how they are affected by geometries and operational parameters, and to compare the simulated outlet losses to current outlet loss model outputs to determine their validity and suggest improvements.

II. Approach

The authors have developed a two-phase, three-dimensional, transient, dynamically meshed CFD model with OpenFOAM 4.0 (The OpenFOAM Foundation Ltd., London, United Kingdom) to accurately approximate the behavior of ASGs during operation for a wide range of geometries and operating conditions.

The flow was modelled with the RANS equations and the Boussinesq eddy viscosity assumption. A two-phase, volume of fluid approach was used to model the free surface, and Menter's Shear Stress Transport (SST) method [9] was used for turbulent closure. The SST turbulent closure method

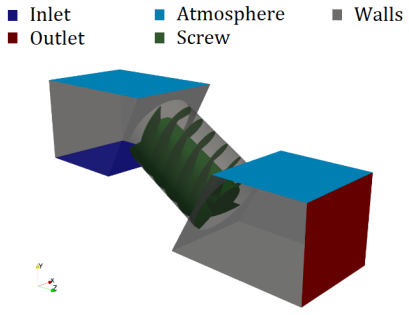

Figure 2. CFD simulation domain.

Table 1. Dimensions and operating parameters of simulated screws.

Screw Number	Scale	D_i (m)	D_o (m)	D_h (m)	L (m)	S (m)	N (-)	β (°)	G_w (m)	n (-)	Ω (rev min^{-1})	Q (m^3 s^{-1})
1	0.469	0.0789	0.148	0.0347	0.572	0.149	3	24.5	0.002	0.014	57.5	0.00115
2	1.00	0.168	0.316	0.0740	1.22	0.318	3	24.5	0.002	0.014	50.0	0.00827
3	2.13	0.359	0.675	0.158	2.60	0.678	3	24.5	0.004	0.014	44.8	0.0699
4	3.16	0.532	1.00	0.234	3.86	1.00	3	24.5	0.006	0.014	40.0	0.202
5	6.33	1.06	2.00	0.468	7.71	2.01	3	24.5	0.008	0.014	31.5	1.23
6	11.1	1.86	3.50	0.819	13.5	3.51	3	24.5	0.010	0.014	21.7	4.51
7	15.8	2.66	5.00	1.17	19.3	5.02	3	24.5	0.010	0.014	17.1	10.3

allowed for the application of Wilcox's k-ω model [10] in near-wall regions with lower Reynolds numbers, and the k-ε model [11] in the free-stream region when Reynolds numbers are higher. The advantage of this method is that it applied both models in the regions they respectively perform best. The choice of the SST method was also due to the relative importance of mesh size in the problem, and because the model is most commonly used for hydro turbine modelling.

An Euler scheme was used for time discretization. Gradient and Laplacian discretization was accomplished with second order central schemes. The divergence of velocity was discretized using second order upwind. An adaptive timestep was used to maintain an acceptable Courant number, with typical timestep values on the order of 10^{-4} s.

Model evaluation was shown in a previous study submitted for publication [12]. The model has been compared to data gathered from seven different sized ASGs with outer diameters of D_o = 0.150, 0.316, 0.381, 1.39, 2.50, 2.90, and 3.60 m, so it is suggested to be an accurate approximation of the power production and power loss phenomenon observed in all sizes of screws. After validation, the model was used to extend the literature's data to include larger sized screws with various geometries and operating parameters. The CFD simulation allowed for data to be gathered from any imaginable Archimedes screw configuration – something that is not economically feasible or practical in the real-world.

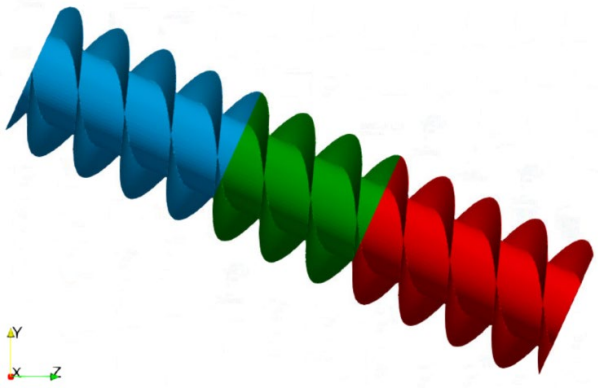

Figure 3. Inlet section (left, blue), ideal section (center, green), and outlet section (right, red) of the screw within the CFD domain.

A set of simulations were run for seven different scale-sizes of a well-tested laboratory screw (screw 2 in Table 1). Screw 2 was the most-tested screw at the University of Guelph's Archimedes screw laboratory. By simulating geometrically identical, scale-sized versions of screw 2, the authors were able to observe the impact that length-scale had on the contributing factors of power production and loss during operation.

In this study, the authors simulated the effects of varying outlet submergence (ψ_L) for each of the seven scaled screws operating at a fill height of f = 1. A full range of submergence from ψ_L = 0 to 1 by increments of 0.1 was simulated for screws 2 and 5. The initial results of these simulations were reviewed and, to be computationally economic, the remaining screws were simulated with outlet submergences of ψ_L = 0.2, 0.5, 0.6, and 0.7. Curves were then developed for outlet submergence with respect to each scale-size to see how outlet submergence and length-scale effected outlet loss.

The CFD model measures power production by calculating the forces on the screw's blades due to hydrostatic pressure and viscous pressure. The forces are then taken as moments about the screw's axis of rotation to determine the mechanical torque contribution due to hydrostatic pressure (the "power producing torque") and viscous pressure (the "friction loss torque"); the difference between the two torque values is the mechanical torque at the generator's gearbox shaft.

To calculate outlet loss, the screw was divided into three segments: the inlet section, ideal section, and outlet section according to Figure 3. The ideal section constituted one full pitch-length in the middle of the screw. The authors suggest that in a long enough screw, the buckets in the middle of the screw would become independent of inlet and outlet effects. The power produced by this middle section is therefore the idealized power production in a screw. The remaining length of the screw was then partitioned into two equal segments: the inlet section at the top, and the outlet section at the bottom.

To measure the outlet loss, the power production was calculated in each of the sections as shown in Figure 4 for screw 2 (cf. Table 1). The figure has three subplots. The hydrostatic pressure component of power is shown in the top left plot, the viscous component of power is shown in the top right plot, and the total power (the difference between the

two) is shown in the bottom plot. Power is presented across the range of outlet submergence levels for the inlet section, ideal section, and outlet section. The resultant power is also shown, it is the summation of the three sections. The ideal (scaled) data represents the total power production if the ideal section were scaled to the entire screw length.

The outlet effects are found similarly to the "ideal (scaled)" data points. The ideal section is scaled to the outlet length, and the difference between the outlet section and the scaled ideal section torque is equal to the effects of the outlet.

III. Results

Figure 4 showed that the inlet section and ideal section consistently produced the same power level throughout the range of submergence levels – except for the data point at a submergence of $\psi_L = 1$. This suggested that the inlet and middle of the screw were not significantly impacted by the effects of the screw's outlet. The outlier data point at $\psi_L = 1$ was due to the simulation geometry. The CFD model used in this study consisted of a screw between an upper and lower basin, enclosed in a pipe (cf. Figure 2). The simulation used a two-phase solver to approximate what was effectively a complex open-channel flow problem. However, when the submergence level reached $\psi_L \geq 1$, the pipe became closed at the outlet, created an unrealistic backpressure in the system and biasing the results. The authors suggest that the simulations are valid up to an outlet submergence of about $\psi_L \approx 0.9$, after which the simulation transitions from the realistic open-channel case, to a complex, partially-filled pipe flow problem.

While the inlet and ideal sections remained constant in Figure 4, the outlet section power production changed drastically throughout the range. In a theoretically ideal screw that is free of outlet loss, lower submergence levels correspond to a higher overall head drop, and so power production should be higher. Conversely, higher submergence levels correspond to lower power production.

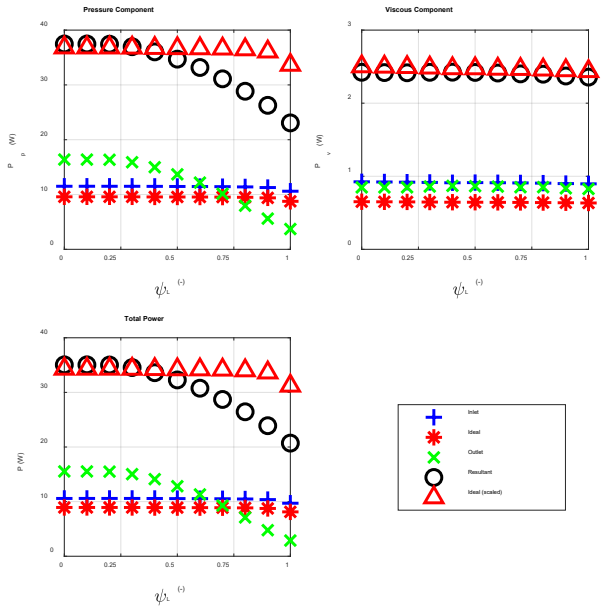

Figure 4. Power production across the range of outlet submergence for the inlet section, ideal section, and outlet section as well as the total power production and the ideal, scaled total power.

Using Nuernbergk's [2] relationships, screw 2 (and subsequently all screws in Table 1) have an optimal lower submergence level of $\psi_L = 0.605$. The cases of higher-than-optimal submergence seem to have a very predictable decreasing trend, and behave as expected with regards to the theoretical case. However, in the low-level submergence case, there seems to be a plateau of power production from $\psi_L = 0$ to 0.3. This indicates that the screw becomes much less efficient in the low-level case, since the theory would dictate an increasing trend in power production as submergence decreases.

To visualize the effects of the outlet further, the difference between the outlet section torque and the scaled ideal section were found. The ideal section was scaled to the length of the outlet section as follows.

$$P_{id_o} = \frac{L_o}{L_{id}} P_{id} \tag{7}$$

Where the power production of the ideal section (P_{id}) is multiplied by the length of the outlet section (L_o) and divided by the length of the ideal section (L_{id}) to find the ideal power production scaled to the length of the outlet (P_{id_o}). The difference between the outlet section power production and this scaled ideal section power was then plotted across the range of outlet submergence (Figure 5). Note that the left axis corresponds to the power difference for screw 2, and the right axis corresponds to screw 5 (cf. Table 1).

Interestingly, the plot shows that the difference in power between screw 2 and screw 5 is almost perfectly scaled by a magnitude of 1000. With some manipulation of dimensional analysis, the dimensionless scaling term below was developed:

$$\Pi_{L_o} = \frac{\Delta P_{L_o}}{\rho g \omega D_o^4} \tag{8}$$

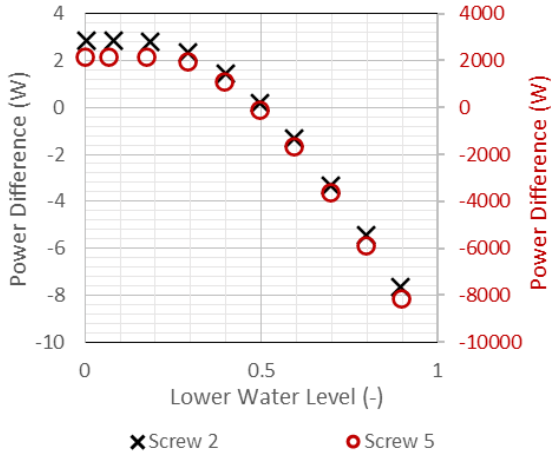

Figure 5. Power difference between the outlet section torque and the scaled ideal section torque for screw 2 (black, left axis), and screw 5 (red, right axis).

The term can be taken for screw 2 and screw 5 and conflated to yield the following:

$$\Pi_{L_{O_2}} = \Pi_{L_{O_5}} \tag{9a}$$

$$\frac{\Delta P_{L_{O_2}}}{\rho g \omega_2 D_{o_2}^4} = \frac{\Delta P_{L_{O_5}}}{\rho g \omega_5 D_{o_5}^4} \tag{9b}$$

$$\frac{\rho g \omega_5 D_{o_5}^4}{\rho g \omega_2 D_{o_2}^4} = \frac{\omega_5 D_{o_5}^4}{\omega_2 D_{o_2}^4} = 1007.3 \tag{9c}$$

The agreement between the results and the magnitude of this coefficient suggests that the outlet power loss scales by the diameter to the fourth power and rotation speed directly. However, it is important to note that these screws are geometrically identical except for scale-size; they have the same inclination angle (β), number of blades (N), diameter ratio (D_o/D_i), pitch diameter ratio (S/D_o), and length ratio (L/S). A final version of the model must account for these variations.

As Figure 5 demonstrates, quantifying outlet loss is difficult, especially since it appears to be a power gain in low-submergence levels due to the increase in available head. So, the authors propose a method to quantify the loss as the "unrealized outlet power loss". In cases when submergence is non-optimal (i.e. low- or high-levels), the outlet section length for Eq. 7 needs to be modified to the "outlet section length for optimal submergence". The adjusted outlet length can be calculated as:

$$L_o' = L_o + \frac{D_o \cos\beta}{\sin\beta}\left(\psi_L' - \psi_L\right) \tag{10}$$

The power loss was also non-dimensionalised by the diameter and rotation speed:

$$\Pi_{L_o} = \frac{L_o'}{L_{id}} \frac{P_{id}}{\rho g \omega D_o^4} \tag{11}$$

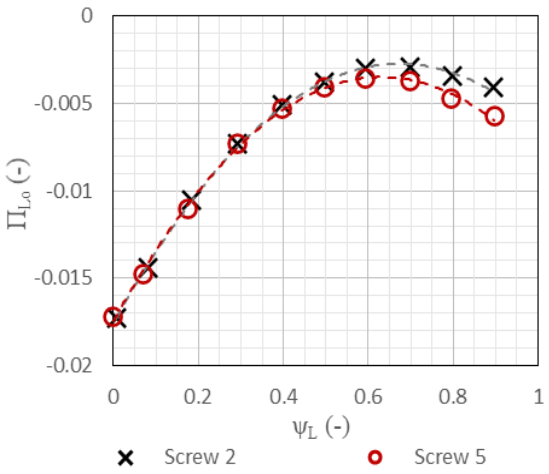

Figure 6. Dimensionless unrealized outlet power loss.

Then, Figure 5 was recast in dimensionless terms (Figure 6). In Figure 6, the unrealized outlet power loss is always a negative value and is lowest near the optimal submergence level – suggesting that this is a reasonable method to observe outlet loss. The dimensionless unrealized outlet loss curve looks similar to a quadratic curve, suggesting a strong second-order relationship between outlet submergence and power loss. A second order polynomial curve was fit to each data range to help visualize the results; the agreement of the fitted curve corroborates this analysis.

Following up on this trend, the five-remaining scale-size screws were simulated for outlet submergence levels of ψ_L = 0.2, 0.5, 0.6, and 0.7 to save computational time and capture the range of interest. The results of the unrealized outlet power loss versus the normalized outlet submergence level is shown for the range of scale-size screws in Figure 7. The normalized submergence level is the submergence level minus the optimal submergence level of each simulation.

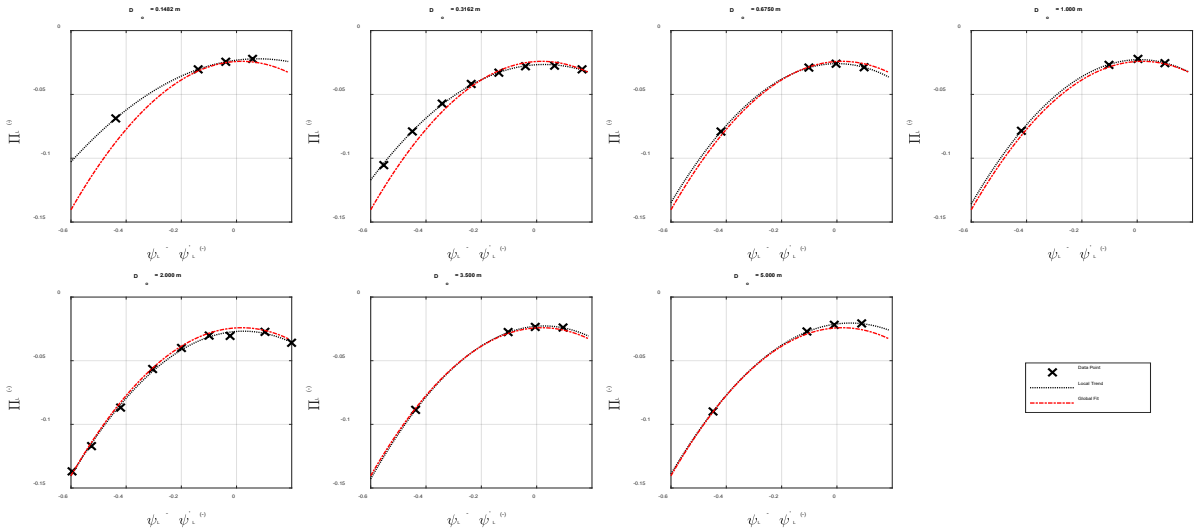

Figure 7. Dimensionless unrealized outlet power loss by the normalized outlet submergence level shown against a local 2nd order polynomial fit and a "global" 2nd order polynomial fit based on the 5 real-scale screws.

Figure 7 shows that the scaling parameters work remarkably well – all seven screws fit the global trend reasonably. The two laboratory-scale screws (D_o = 0.1482 and 0.3162 m) saw the least agreement with the global trend, but the five "real-scale" screws (D_o = 0.675, 1, 2, 3.5, and 5 m) seemed to all fit the trend very well. The second order polynomial fit that is shown in Figure 7 as the "global fit" is:

$$\Pi_L = \frac{-303.6\left(\psi_L - \psi_{L_{opt}}\right)^2 + 11.440\left(\psi_L - \psi_{L_{opt}}\right) - 24.192}{1000} \quad (12)$$

Some preliminary work has revealed that the outlet loss has a dependency on the number of blades (N), the inclination angle (β), and the fill height of the screw buckets (f) during operation. So, the authors suggest equation 8 should be revised to have corrective terms for each phenomenon (λ_N, λ_β, and λ_f, respectively).

$$\Pi_{L_o} = \frac{1}{\lambda_N \lambda_\beta \lambda_f} \frac{P_{L_o}}{\rho g \omega D_o^4} \quad (13)$$

The function corresponding to each correction factor may take a different form than is suggested in equation 1 – work is currently underway to quantify these scaling factors.

IV. Conclusions

The simulations and data outlined in this article provide novel insight into outlet loss in Archimedes screw generators. Data quantifying outlet loss in ASGs does not exist in the literature and is an integral factor for future outlet model development. Scaling and non-dimensionalisation yielded surprising results. It was theorized that outlet loss would scale by a function of the rotation speed and the fourth order diameter, however the results suggest that there is a nearly direct correspondence between the two for these simulations.

Further simulations are underway that vary the number of blades, inclination angle, and fill height of the screw to observe how the "global" 2nd order polynomial fit performs. The current hypothesis is that each of these parameters will alter the relationship between normalized outlet submergence and dimensionless unrealized outlet power loss (cf. Figure 7) in some way – possibly shifting the vertex, changing the amplitude, or widening the parabola.

Acknowledgment

Aspects of this work were financially supported by the Natural Sciences and Engineering Research Council (NSERC) Collaborative Research and Development (CRD) program (grants CRDPJ 433740-12 and CRDPJ 513923-17) and Greenbug Energy Inc. (Delhi, ON, Canada). The assistance of Tony Bouk and Brian Weber of Greenbug Energy Inc. is gratefully acknowledged.

References

[1] Karl-August Radlik, "Hydrodynamic screw for energy conversion - uses changes in water supply to regulate energy output," DE4139134A1, 28-Nov-1991.

[2] D. M. Nuernbergk, *Wasserkraftschnecken - Berechnung und optimaler Entwurf von archimedischen Schnecken als Wasserkraftmaschine (Hydropower screws - Calculation and Design of Archimedes Screws used in Hydropower)*, 2nd ed. Detmold: Verlag Moritz Schäfer, 2020.

[3] W. D. Lubitz, M. Lyons, and S. Simmons, "Performance Model of Archimedes Screw Hydro Turbines with Variable Fill Level," *J. Hydraul. Eng.*, vol. 140, no. 10, pp. 1–11, 2014.

[4] J. Rohmer, D. Knittel, G. Sturtzer, D. Flieller, and J. Renaud, "Modeling and experimental results of an Archimedes screw turbine," *Renew. Energy*, vol. 94, pp. 136–146, 2016.

[5] A. Kozyn and W. D. Lubitz, "A power loss model for Archimedes screw generators," *Renew. Energy*, vol. 108, pp. 260–273, 2017.

[6] K. J. Songin and W. D. Lubitz, "Measurement of fill level and effects of overflow in power-generating Archimedes screws," *J. Hydraul. Res.*, vol. 57, no. 5, pp. 635–646, 2018.

[7] D. M. Nuernbergk and C. Rorres, "An Analytical Model for the Water Inflow of an Archimedes Screw Used in Hydropower Generation," *J. Hydraul. Eng.*, vol. 139, no. 2, p. 120723125453009, 2012.

[8] A. Passamonti, "Investigation of energy losses in laboratory and full-scale Archimedes screw generators," Politechnico di Milano, 2017.

[9] F. R. Menter, "Two-equation eddy-viscosity turbulence models for engineering applications," *AIAA J.*, vol. 32, no. 8, pp. 1598–1605, 1994.

[10] D. C. Wilcox, "Formulation of the k-ω Turbulence Model Revisited," in *45th AIAA Aerospace Sciences Meeting and Exhibit*, 2008.

[11] B. E. Launder and D. B. Spalding, "The numerical computation of turbulent flows," *Comput. Methods Appl. Mech. Eng.*, vol. 3, no. 2, pp. 269–289, 1974.

[12] S. Simmons, C. Elliott, M. Ford, A. Clayton, and W. D. Lubitz, "Archimedes screw generator powerplant assessment and field measurement campaign," *Energy Sustain. Dev.*, 2021.